J Mater Sci: Mater Med (2011) 22:1975–1983
DOI 10.1007/s10856-011-4359-7

Particle size and shape effects in medical syringe needles: experiments and simulations for polymer microparticle injection

Mark A. Whitaker · Paul Langston · Andrew Naylor · Barry J. Azzopardi · Steven M. Howdle

Received: 3 February 2011 / Accepted: 24 May 2011 / Published online: 11 June 2011

Abstract Injection of polymeric microparticles is the final step in the drug delivery process. Experience has shown that blockage of the syringe mechanism can be a problem under certain conditions leading to poor control of the final product. Particle size and shape are postulated to be significant factors. In this article 2D Discrete element model (DEM) simulations of circles and semi-circles are used to demonstrate the effect of shape on blockage of the syringe mechanism. To corroborate the calculations, a range of experiments on glass spheres and polymers show good agreement with simulations of normally distributed particle sizes. A similar scenario is also briefly modelled in 3D DEM showing similar trends.

1 Introduction

1.1 Medical microparticles

Medically approved polymers are commonly used to prepare drug encapsulated microparticles for subcutaneous injection into the human body [1]. Such particles are usually but not always spherical and are made by double emulsion [2] and spraying techniques [3]. Often overlooked is the administration of these microparticles, via hypodermic syringe with a medical gauge needle. The microparticles are suspended in a liquid injection vehicle (usually a low viscosity aqueous solution such as carboxymethyl cellulose solution) and are injected under the skin or intramuscularly. Large needle sizes are typically employed in these procedures to eliminate the possibility of blockages. However this approach is cautious, when perhaps smaller needle sizes could be used to improve patient comfort. For this reason this study investigates the effects of particle shape and size in order to understand the key factors that influence particle passage through a needle orifice.

Two main types of particle shape are investigated, spherical and hemispherical; to see what effect they have in terms of blockage (Fig. 1). In both cases, the particles have been fabricated using the Particles from gas saturated solution technique (PGSS), where supercritical carbon dioxide ($scCO_2$) under mild temperatures and pressures has been used to atomise the medical polymer poly(lactic-co-glycolic acid), PLGA. Drug particles can be added in this process to create sustained release formulations [4] but have not been attempted for this study.

In this article we explore the effect of particle size and shape upon injectability. Modelling is performed in 2D (and some in 3D) using the DEM approach where model particles were based upon circles and semi-circles. The key target was to determine the injectability of spherical and hemispherical particles through medical gauge slip-tip needles. Commercially these are described as 19 & 21G. These have outer diameters of 1.07 and 0.83 mm, respectively and are large and painful for patient injection. Smaller gauge needles (23 and 25G) are of 0.64 and 0.52 mm diameters [5], and are much less intrusive and

M. A. Whitaker · S. M. Howdle (✉)
School of Chemistry, University of Nottingham, University Park, Nottingham NG7 2RD, UK
e-mail: steve.howdle@nottingham.ac.uk

P. Langston · B. J. Azzopardi
Faculty of Engineering, Chemical and Environmental Research Division, University of Nottingham, University Park, Nottingham NG7 2RD, UK

A. Naylor
Critical Pharmaceuticals Limited, BioCity Nottingham, Pennyfoot Street, Nottingham NG1 1GF, UK

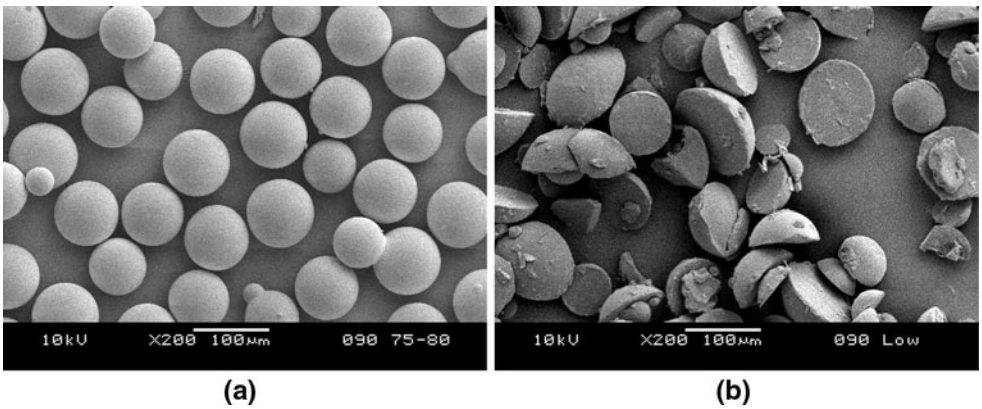

Fig. 1 **a** SEM of glass spheres sieved in the nominal range 75–80 µm. **b** PLGA hemispheres sieved in the nominal range <100 µm

painful for the end user. Thus this study focuses upon the requirements to obtain a clean injection without particle blockage for the range of needle gauges and particle sizes mentioned. The DEM modelling and experimental behaviour observations are compared. One key balancing factor is that drug delivery formulation particles are required to be as large as possible to minimise drug burst release. The question remains what is the smallest needle required for the largest possible particle size that can minimise discomfort but prevent a dose dump effect after injection?

It has also been found that varying the lactide and glycolide content in PLGA can vary the contact angle that a hemisphere forms post PGSS production, which may in turn affect the flow-ability of the end particles when injected (Fig. 2). Two variants have been discovered: firstly particles with a contact angle of 66 ± 6° have been formulated with PLGA in a 50:50 ratio of lactide to glycolide; secondly hemispheres with a contact angle of 89 ± 11° have been measured [6] with a PLGA ratio of 100:0, which is in fact polylactic acid, PLA. These shapes are approximated to 60° and 90° for initial investigation. All experimental particles are assumed to be 90° in contact angle.

The study is also extended to look briefly at the effect of 3D spherical and hemispherical particles in DEM.

1.2 Objectives

This study compares results of polygon DEM 2D simulations with experiments on syringe flow in terms of whether blockage occurs. It is recognised that 2D has significant limitations but previous studies [7, 8] have shown it to be useful in initial assessments. Some comparable 3D simulations are also considered in less detail. Several techniques to model non-spheres are evolving in DEM as reviewed by Dziugys and Peters [9] and in Li et al. [10], Fraige et al. [7]. The main objectives here are to consider the validity of DEM for syringe blockage and how it might be utilised practically.

2 Materials and methods

2.1 Materials

PLGA RG502H (13 kDa) was purchased from Boehringer (Ingelheim, Germany). Pharmaceutical grade CO_2 (99.99%)

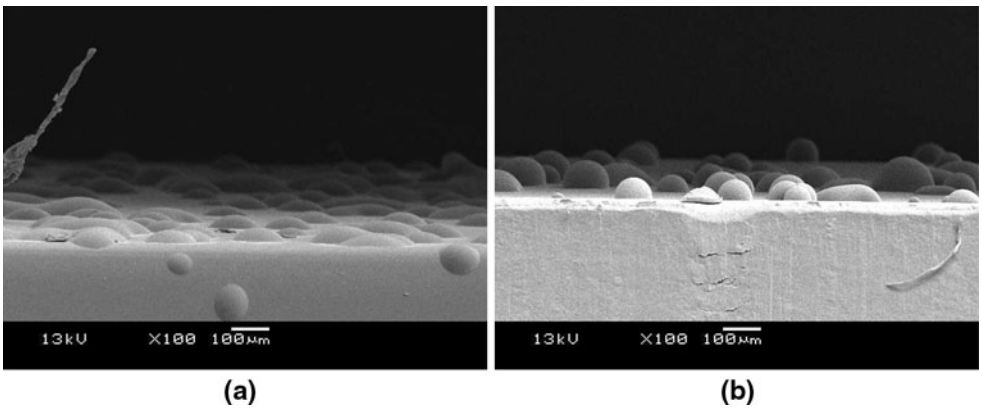

Fig. 2 Contact angle variation as a function of lactide content. **a** 50% lactide. **b** 100% lactide. Measurements taken with ImageJ using the low bond axisymmetric drop shape analysis plug-in [6]

and zero grade N_2 were supplied by BOC (Nottingham, UK). All high pressure stainless steel pipes and connectors were from Swagelok (Manchester, UK). Micron sized glass beads were also used (Nottingham University).

2.2 Particle production

The PGSS technique uses the weak solubility of $scCO_2$ to mix polymers. The supercritical gas lowers the melting or glass transition temperature of polymers causing them to form a gas saturated solution [11]. The procedure involves use of a high pressure vessel. Polymer and CO_2 are added and the temperature and pressure are raised to above the critical point conditions (31.1°C & 73.8 bar). This causes the polymer to liquefy. The plasticised mixture is then stirred to enable mixing with any drug additives. The polymer/drug mixture is atomised through a nozzle generating particles [12] which are collected in a cyclone downstream of the device. On spraying, the CO_2 evaporates causing the melting/glass transition temperature to rise again. This solidifies the polymer, creating the shape of the particles that would eventually be injected into a patient.

The PGSS technique produces spherical and near spherical particles. Near perfect spheres are produced in quantities of less than 100 mg per 2 g batch, for this reason glass beads are used in the experimental section of this article as their shape was guaranteed spherical (Fig. 1).

Standard PGSS particles can be further processed to make hemispheres. A hemispherical particle is a PGSS particle that has undergone secondary plasticisation. This is achieved by spreading the particles out on Teflon® sheets, re-exposing them to CO_2 in a pressure vessel, depressurising and sieving the correct fraction for injection. The hemispheres produced are shown in Fig. 3, they are smooth, non-porous and are of a sufficient number in the batch making process to be experimented upon for this article.

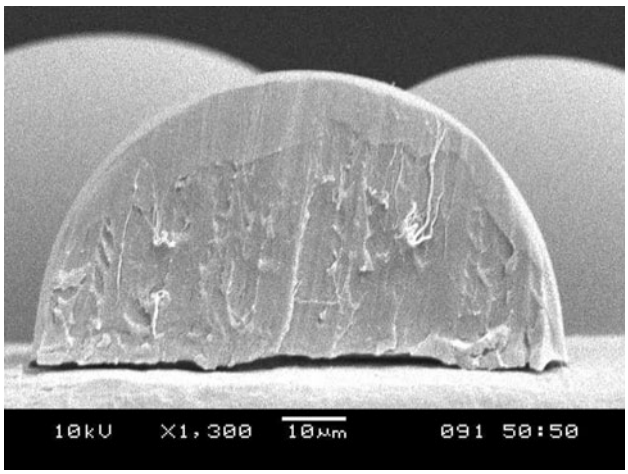

Fig. 3 SEM image of hemispheres with sliced example showing internal structure

2.3 Injection testing procedure

An injection force of 10 N is considered to be the upper limit value acceptable for a 1 ml syringe [13]. If this value was exceeded then the injection was deemed a blockage. 1 ml slip-tip disposable syringes and matching needles (BD & Co, Franklin Lakes, USA) were used in the experimental with a TA HD Plus texture analyser (Stable Micro Systems, Goldaming, UK) to measure the force of injection as a function of syringe plunger movement. This is shown in Fig. 4.

The particles were suspended in an injection vehicle (Water with 1.5% Carboxymethyl cellulose, 0.9% Sodium Chloride), with a dose of 200 mg/ml. The temperature of the injection vehicle was controlled at 10°C giving a viscosity of 0.13 ± 0.01 Pa.s. Three repeats were taken for each sample tested.

2.4 Experiments for DEM comparison

Monodisperse and normal distributions were simulated using DEM. Distributions were then experimentally tested

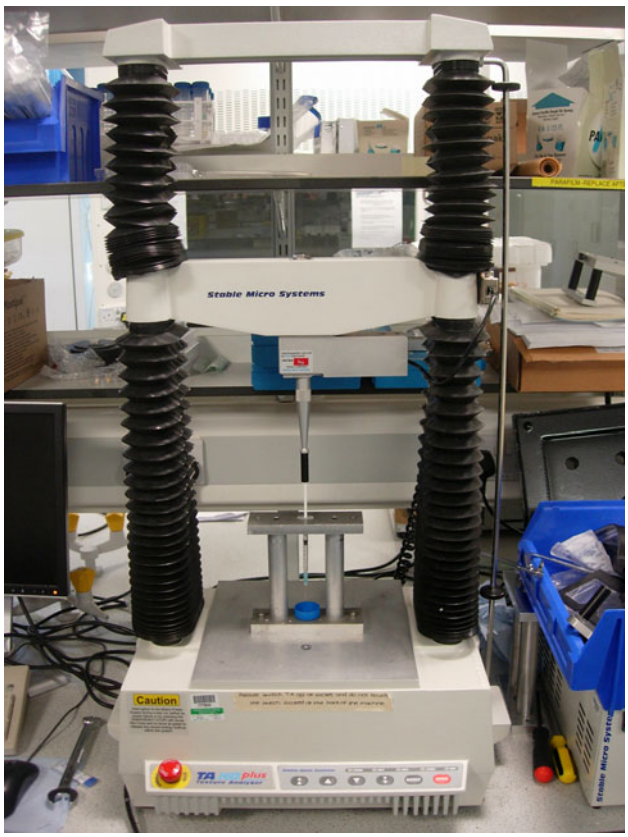

Fig. 4 Texture analyser apparatus used for injectability studies

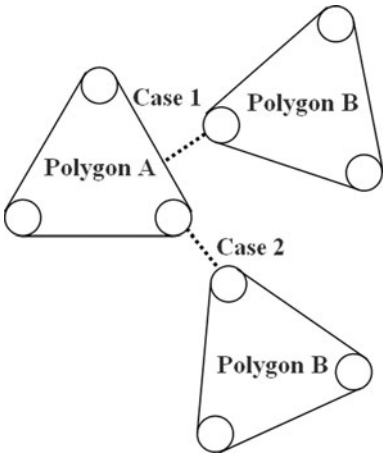

Fig. 5 Polygon contact model showing vertex circle-boundary line contact (Case 1) and inter-vertex circle contact (Case 2)

with a 23G needle attached to 1 ml syringes. To facilitate the experiments glass spheres were used in a variety of sieved distributions, whereas polymer hemispheres were made using the secondary plasticisation process. The size range of the nominal sieved fractions were more accurately measured using laser diffraction, specifically a Helos/BR (Sympatec, Clausthal, Germany) and were approximated by normal distributions truncated between d_{10} and d_{90} to describe 80% of the particle population in the simulation as the DEM program required defined boundaries for it to work within a reasonable time limit.

2.5 DEM 2D model

2.5.1 Sphere 2D model

The basic form of this DEM model [8] is fairly standard with a linear spring and dashpot contact mechanics approach and has been applied here to silo flow to mimic the syringe. It is essentially a 2D model with a fixed particle thickness in the 3rd dimension. It uses an explicit time stepping approach to numerically integrate the motion of each particle from the resulting forces acting on them at each timestep. The inter-particle and particle wall contacts are modeled using the spring–dashpot–slider analogy with rolling friction. Contact forces are modeled in the normal and tangential directions with respect to the line connecting the particles centres. Further details can be found in Fraige et al. [8].

2.6 Polygon 2D model

A representation of the polygon particle model and potential contact types is shown in Fig. 5. Defining the particle contact with perfect polygons can be difficult in some situations. Since real granular materials do not have perfect vertices a small circle is located at each vertex as shown. Each convex polygon is defined by a number of different radial distances from a reference point at specified angles such that the outer angle at each vertex is always greater than 180°. To determine whether two particles interact the separation distance needs to be calculated. This algorithm incorporates calculating the distance from a vertex in polygon B to the boundary line of polygon A with two possibilities as shown in Fig. 5, vertex circle-boundary line contact and inter-vertex circle contact.

2.7 Application of model to syringe flow

An example of the polygon DEM model used here to model the hemispheres is shown in Fig. 6b, c. In this study cohesion is negligible, contact damping is assumed to be quite high due to the interstitial liquid and a moderate value of friction is assumed. Gravity flow is used to replicate the syringe flow. The side walls of the DEM vessel are at 4° to vertical measured from a 23G needle cross-section (BD

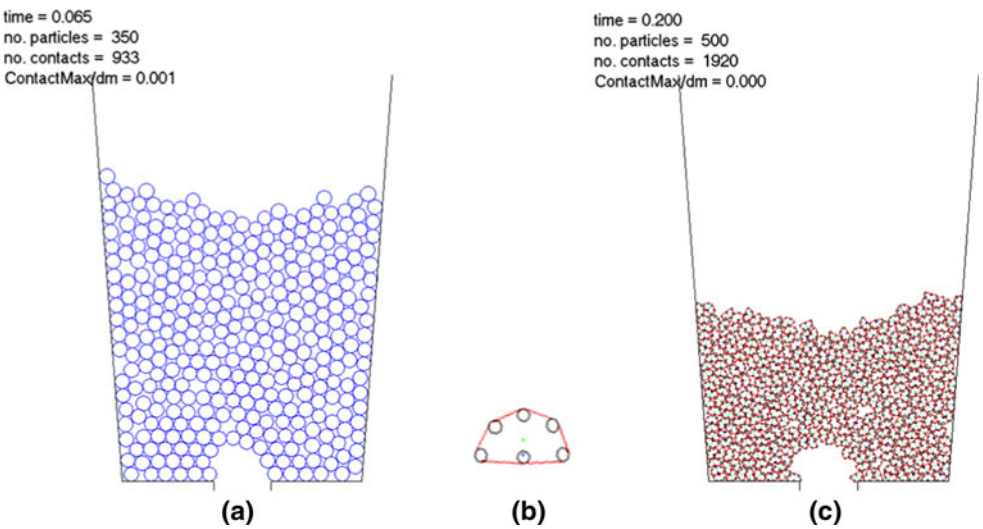

Fig. 6 Snapshot of 2D DEM model replicating syringe flow showing blockage of circles (**a**) and semi-circles (**c**) in 23G needle, and close-up of modelling polygon (**b**)

Table 1 Principal DEM data used in 2D polygon model

DEM parameters	Values
Number of particles	70–800
Example particle diameters (cm)	
Circle	0.00548
90° Contact angle	0.00775
60° Contact angle	0.01000
Density (g/cm^3)	1.3
Friction coefficient	0.5
Particle tangential stiffness, (dyn/cm)	10,000
Particle normal stiffness, (dyn/cm)	10,000
Normal damping coefficient (dyn s/cm)	0.05

Microlance^{TM} 3). The major assumption here is that the phenomenon of blockage is dominated by the solid phase, namely size and shape of the particles. Fluid drag effects are not modelled here. These would add an extra driving force to the particles, but essentially when the particles block it is assumed that they will not be dislodged by this extra force. The principal DEM data are shown in Table 1.

3 Results and discussion

3.1 2D-model and experimental results

3.1.1 Mono-sized simulation

19, 21, 23 & 25G needles were modelled with circles, 60° and 90° contact angle particles. For each needle and shape the blocking point was found. This involved selecting a particle size and either increasing or decreasing the diameter in order to find the limit at which particles could not flow—this was achieved to the nearest micron and assigned as the critical particle diameter, d_p.

Table 2 shows the critical particle diameter required to just cause a blockage for the simulations of near mono-sized systems. For circles the ratio of orifice, B, to d_p had an average of 3.7 ± 0.4 over the four needle types used. For 90° contact angle particles (semi-circles) this ratio reduced to 2.9 ± 0.3 meaning that larger semi-circle diameters can pass through a given gauge needle.

However, by equating d_p of semi-circles to, d_e the diameter of a circle with equivalent area, shows that the semi-circles are more likely to block in terms of particle size based on area i.e. amount of material in the particle. A further simulation with 60° contact angle particles using a 23G orifice shows it is more likely to cause blockage based on d_e. (Note that these 2D simulations have a fixed length in the third dimension, hence equivalent area is the same as equivalent volume. The circles are in fact discs restricted to planar motion.)

The flow characteristics of circles and partial circles with contact angles of 60° and 90°, Fig. 7, were studied in a simulation campaign. The three particles had equal areas. The results showed that they all flowed through the 23G needle simulation geometry but with different flow rates as illustrated in Fig. 8. The 90° partial circles flowed fastest whilst the circles were the slowest. This is somewhat counter-intuitive given the conclusions on blockage above. It shows that particle flow is a complex phenomenon. However, a recent theoretical study [14] showed that frictionless "needle shapes" in 2D flow faster than equivalent circles.

Table 2 2D DEM predictions for blockage of circles, semi-circles and 60° contact angle particles for four common medical gauge needles

Needle		Circles		90° Contact angle (semi-circles)				60° Contact angle particle			
Gauge	B (μm)	d_p (μm)	B/d_p	d_p (μm)	B/d_p	d_e (μm)	B/d_e	d_p (μm)	B/d_p	d_e (μm)	B/d_e
25	260	67	3.88	88	2.96	62	4.19	–	–	–	–
23	340	91	3.73	112	3.04	79	4.30	115	2.96	63	5.40
21	510	127	4.02	168	3.04	119	4.29	–	–	–	–
19	690	222	3.11	247	2.79	175	3.94	–	–	–	–

B needle inner diameter, d_p critical particle diameter, d_e equivalent area circle diameter

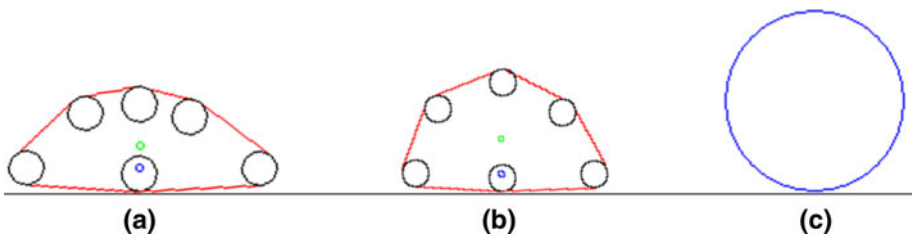

Fig. 7 DEM 2D representation of particles **a** 60° contact angle particle, **b** 90° contact angle particle (*semi-circle*). **c** 180° contact angle particle (*circle*). All with equivalent areas and arbitrary scale particle diameters of 100, 77.5 and 54.8 μm, respectively

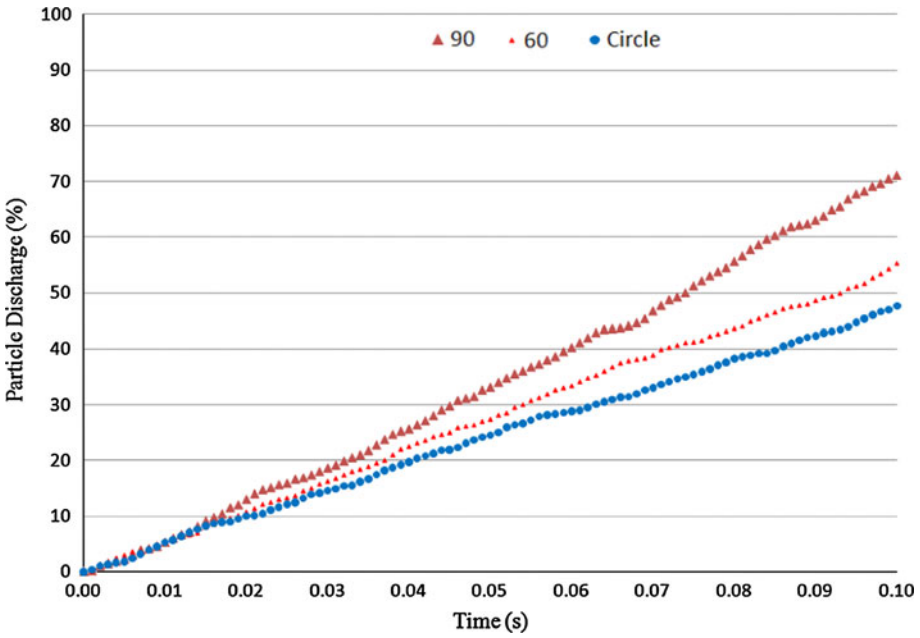

Fig. 8 2D DEM flow comparison between 60 and 90 (*semi-circle*) and 180° (*circles*) contact angle particles. Each particle has equivalent area (Fig. 7)

Table 3 Comparison of 2D DEM and experiment for a range of glass sphere distributions through a 23G needle—d_{10} 10% of particles below this size, d_{90} 90% of particles below this size

Nominal sieve range (μm)	d_{10} (μm)	d_{90} (μm)	DEM	Experiment
Set I: 75–80	50.32	85.47	Flow	3× Flow
Set II: 75–80	62.25	87.66	Block	3× Block

3.1.2 Normal particle size distribution

2D simulations were adapted to account for a distribution of particle sizes. The simulations are compared with laboratory experiments of normal distributions of glass spheres or PLGA hemispheres, testing whether they would flow through 23G needles attached to 1 ml syringes. The semi-circles in the 2D simulations were of the same contact angle as that of the polymer hemispheres, i.e. 90°.

Two sieved fractions of glass spheres were sized (Table 3) using a Helos/BR laser diffraction apparatus (Sympatec, Clausthal, Germany). The first set was regarded as the smaller fraction. The DEM modelling of 2D circles predicted that this sample would flow under all experimental conditions tested. Our measurements using the Texture Analyser confirmed this to be true (Fig. 9). The second set of particles, the larger fraction, was predicted to block and this was proven in the injection tests.

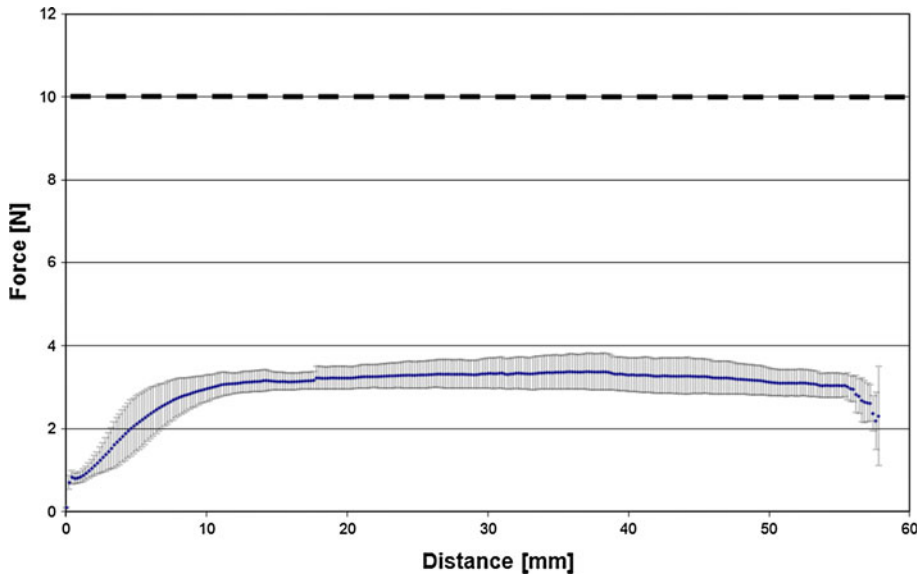

Fig. 9 Successful injection with glass spheres. Experiment result from Table 3 for the size distribution d_{10}: 50.32 to d_{90}: 85.47 μm. *Dashed line* is the acceptability limit

Table 4 Comparison of 2D DEM and experiment for a range of polymer hemisphere distributions through a 23G needle

Nominal sieve range (μm)	d_{10} (μm)	d_{90} (μm)	DEM	Experiment
Set I: <100	35.75	108.94	Flow	2× Flow & 1× Block
Set II: 100–150	35.97	143.96	Block	3× Block

The effect of particle size distribution on the flow of PLGA hemispheres was tested by separating a sample with a wide range of particle sizes into two sub sets by sieving. These were nominally smaller and larger than 100 μm. The two fractions were then sized more accurately by laser diffraction (Table 4). For the smaller sized fraction the simulations predicted a successful flow of particles, this was nearly correct in the experiment as two out of the three samples tested flowed (Fig. 10). The larger fraction was predicted to block and did so with three repeats.

The results from Table 3 shows that 2D DEM gives good predictions for the glass spheres and reasonable agreement for polymer hemispheres (Table 4), which is encouraging given the simplifications and assumptions employed in the modelling. These results support the idea that particle geometry is the key factor in blockage.

3.2 DEM 3D model and results

3.2.1 Sphere intersection model

A small number of simulations were carried out with a 3D model. Near-hemispheres have been modelled based on the approach described in Li et al. [10], which has been termed the sphere intersection method. Figure 11 illustrates the principle involved and shows an example contact situation. An example of the model sphere flow here is shown in Fig. 12 and the hemisphere model in Fig. 13. This is similar to the 2D model in that it is gravity flow without interstitial fluid. It is on a larger scale flowing through a square orifice in a flat-bottomed rectangular silo. Hence this is only an illustration of the principle in 3D not a direct model of the syringe. Li et al. [10] describe how this model has been validated against simple laboratory experiments of sphero-disc particles. The principal data are similar to the 2D model in Table 1 except that it is geometrically scaled up to a nominal 1 cm maximum size to facilitate the DEM (allowing a larger time-step). Note the hemisphere is approximated by making one of the component spheres much larger than the other (Fig. 11a).

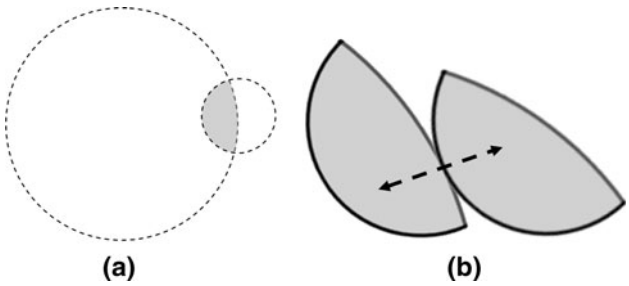

Fig. 11 Principle of the sphere–sphere intersection model. **a** Particle described by region of intersection. **b** 2D representation of contact example and direction of normal force

3.2.2 Model results

The first simulation set investigates the blocking point of spheres and hemispheres as they pass through the square

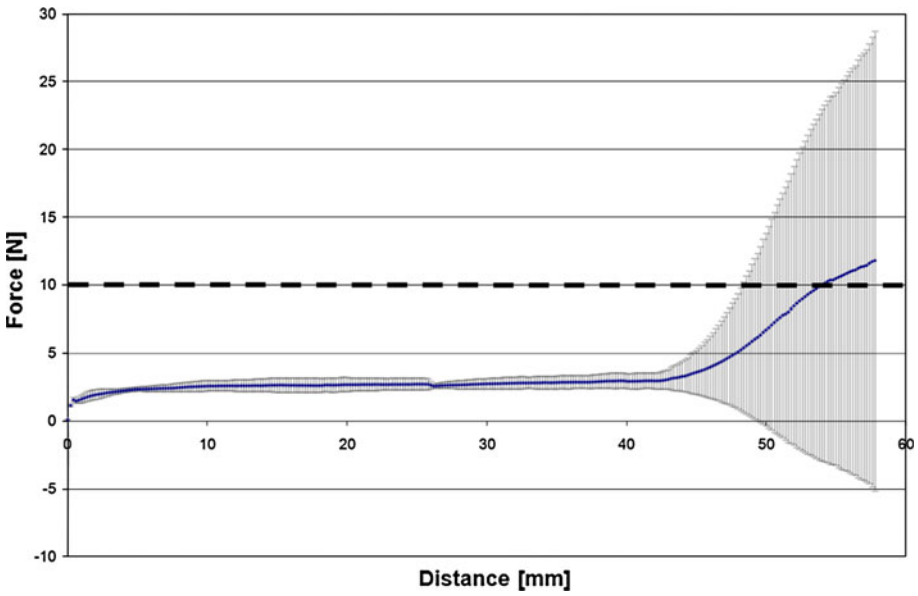

Fig. 10 Blocked injection with PLGA hemispheres. Overall failure. Experiment result from Table 4 for the size distribution d_{10}: 35.75 to d_{90}: 108.94 μm. *Dashed line* is the acceptability limit

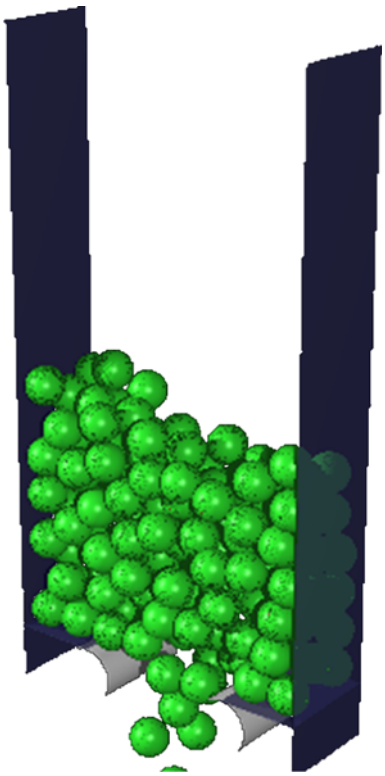

Fig. 12 Example of DEM 3D sphere flow simulation showing discharging case. (Front & back walls not shown for clarity)

orifice. The particle sizes are shown in Table 5. Both types have the same volume, and both are monodisperse. The orifice size was adjusted to find the critical point at which flow stops. The results in Table 5 show that spheres flow through a smaller orifice than the hemispheres. This is consistent with the 2D results shown in Table 2.

Table 5 3D DEM predictions of blockage for square orifice. Here B is the orifice side length

Shape	d_p (cm)	B (cm)
Sphere	0.79	1.82
Hemisphere	1.0	2.10

All particles have the same volume. Number of particles = 300

The second simulation set compares a case where both above particle types flow through the same orifice. The width of the orifice was chosen to be proportional to a 23G needle (noting that the square 23G-based orifice is not the same as the true rounded version). The results in Fig. 14 show that the spheres flow about 5% faster than the hemispheres. The hemispheres show a sudden drop at one point indicating a tendency to blockage. Hence the 3D flow results are consistent with the blockage results unlike the 2D case discussed in Section 3.2.

4 Conclusions and further work

The flow and blocking phenomenon in the syringe injection of polymer microparticles is reasonably represented by the 2D circle and polygon DEM simulations. 2D DEM simulations of near mono-sized particles showed that the semi-circles are more likely to block when compared with an equivalent area circle. Experiments injecting glass spheres and polymer hemispheres gave reasonable agreement with

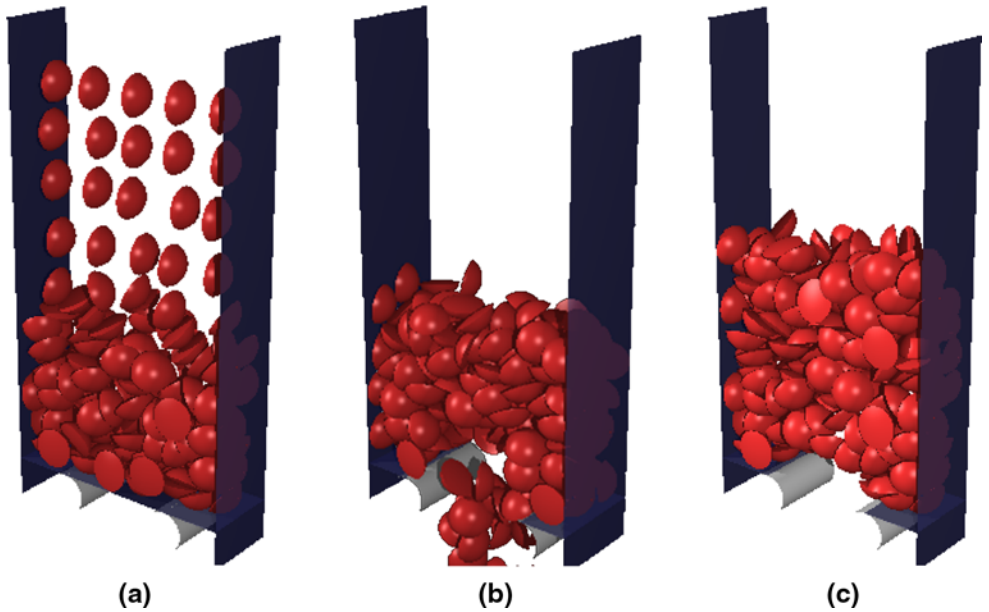

Fig. 13 Example of DEM 3D with hemispheres. **a** Filling. **b** Discharging. **c** Blocked

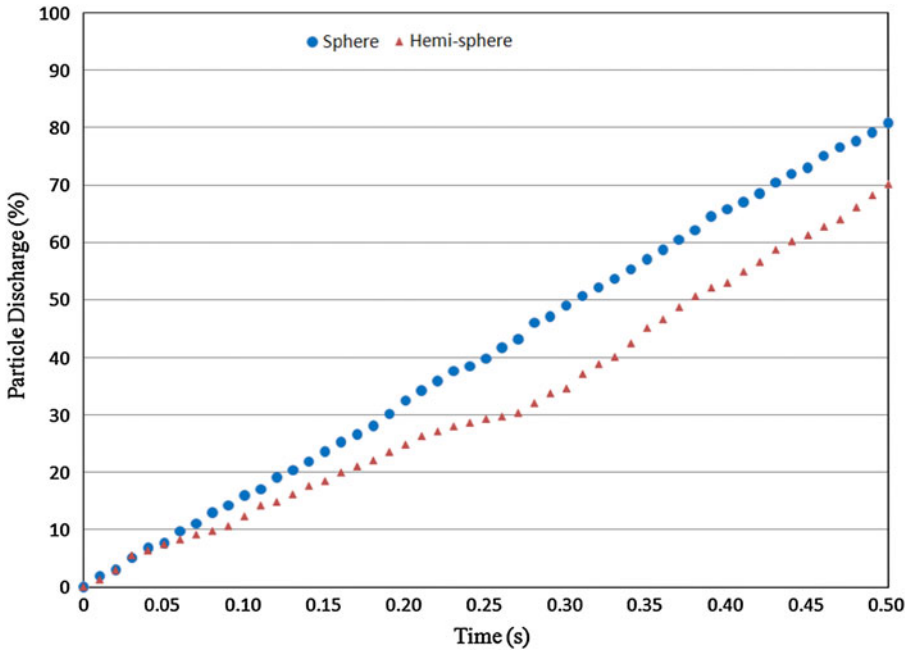

Fig. 14 3D DEM flow comparison between spheres and hemispheres. Orifice side length *B* fixed at 3.40 cm

the DEM distribution simulations. Some comparable 3D DEM modelling flow through a square orifice geometry showed that spheres flowed faster than equivalent volume near-hemispheres with identical material properties.

The contact angle of the hemispheres is a significant factor considering whether a flat or bulbous shape flows more successfully. Further DEM simulations in 3D should investigate these shapes in more detail. These "dry" DEM simulations have the potential to help optimise particle design here.

Acknowledgments We would like to thank the Biotechnology and Biological Sciences Research Council (CASE Studentship BB/F018142/1) and Critical Pharmaceuticals for financial support in this project.

References

1. Rathbone MJ, Hadgraft J, Roberts MS, Lane ME. Modified-release drug delivery technology. 2nd ed. New York: Informa Healthcare; 2008. pp. 263–272
2. Zhang JX, Zhu KJ. An improvement of double emulsion technique for preparing bovine serum albumin-loaded PLGA microspheres. J Microencapsul. 2004;21(7):775–85.
3. Davies OR, Lewis AL, Whitaker MJ, Tai HY, Shakesheff KM, Howdle SM. Applications of supercritical CO_2 in the fabrication of polymer systems for drug delivery and tissue engineering. Adv Drug Deliv Rev. 2008;60(3):373–87.
4. Jordan F, Naylor A, Kelly CA, Howdle SM, Lewis A, Illum L. Sustained release hGH microsphere formulation produced by a novel supercritical fluid technology: in vivo studies. J Control Release. 2010;141(2):153–60.
5. Fisher Scientific Laboratory Catalogue, Needle Gauge Index; 2007–08. p. 396.
6. Stalder AF, Kulik G, Sage D, Barbieri L, Hoffmann P. A snake-based approach to accurate determination of both contact points and contact angles. Colloid Surf A. 2006;286(1–3):92–103.
7. Fraige FY, Langston PA, Chen GZ. Distinct element modelling of cubic particle packing and flow. Powder Technol. 2008;186(3):224–40.
8. Fraige FY, Langston PA, Matchett AJ, Dodds J. Vibration induced flow in hoppers: DEM 2D polygon model. Particuology. 2008;6(6):455–66.
9. Dziugys A, Peters B. An approach to simulate the motion of spherical and non-spherical fuel particles in combustion chambers. Granul Matter. 2001;3(4):231–65.
10. Li JT, Langston PA, Webb C, Dyakowski T. Flow of sphero-disc particles in rectangular hoppers—a DEM and experimental comparison in 3D. Chem Eng Sci. 2004;59(24):5917–29.
11. Yeo SD, Kiran E. Formation of polymer particles with supercritical fluids: a review. J Supercrit Fluids. 2005;34(3):287–308.
12. Hao JY, Whitaker MJ, Wong B, Serhatkulu G, Shakesheff KM, Howdle SM. Plasticization and spraying of poly (DL-lactic acid) using supercritical carbon dioxide: control of particle size. J Pharm Sci. 2004;93(4):1083–90.
13. ISO 7886-1 1993 (E). Sterile hypodermic syringes for single use—Part 1: syringes for manual use.
14. Langston PA, Al-Awamleh MA, Fraige FY, Asmar BN. Distinct element modelling of non-spherical frictionless particle flow. Chem Eng Sci. 2004;59(2):425–35.